

Final report

Multifunctional Polymer Matrices to Direct Virus-free Cell Reprogramming

Leibniz-Institute: Leibniz Institute of Polymer Research Dresden
Reference number: SAW-2011-IPF-2
Project period: 01.05.2011-30.04.2014
Contact partner: Prof. Dr. Carsten Werner

Report
SAW-2011-IPF-2 68
Multifunctional Polymer Matrices to Direct
Virus-free Cell Reprogramming

Carsten Werner, Chair for Biofunctional Polymer Materials, **Leibniz Institute of Polymer Research Dresden (IPF)**, Max Bergmann Center of Biomaterials (MBC) & Technische Universität Dresden, Center for Regenerative Therapies Dresden (CRTD)

in collaboration with (in alphabetical order)

Jens-Uwe Sommer, Chair for Theory of Polymers, Leibniz Institute of Polymer Research Dresden (IPF) & Technische Universität Dresden, Institute for Theoretical Physics,

Elly Tanaka, Chair for Animal Models of Regeneration, Technische Universität Dresden, Center for Regenerative Therapies Dresden (CRTD), and

Yixin Zhang, Junior Group Leader, Technische Universität Dresden, Innovation Center for Molecular Bioengineering (B CUBE)

Project overview & summary

The interdisciplinary research program of the project aimed at utilizing a novel multifunctional polymer matrix system to deliver CPP-fused transcription factors across cell membranes and to present growth factors and adhesion ligands by network structures with tunable and responsive physical and degradation characteristics. Based on this platform, it was planned to explore whether and how the permeation of CPP-fused transcription factors across lipid bilayer membranes can be fortified and if exogenous matrix signals can mediate reprogramming of fibroblasts into induced pluripotent stem (iPS) cells, as well as their subsequent maintenance and differentiation.

To achieve these goals, the research program of our consortium included the expression and chemical modification of transcription factors and the adaptation of a set of peptide-functionalized polyethylene glycol-heparin (starPEG-heparin) hydrogel matrices to modulate their localized presentation as well as the provision of various physical and biomolecular signals. Fundamental principles and interactions determining the permeation of chemically engineered, matrix-delivered transcription factors through lipid membranes were explored through joint theoretical and experimental investigations using lipid bilayer model systems. Closely connected to those activities, the impact of various combinations of engineered matrices and transcription factors on the generation of iPS cells were studied using human and mouse fibroblast cells.

Report

Theoretical studies to explore the permeation of polymers and nano-particles through lipid bilayer membranes (work group of Prof. J.-U. Sommer, IPF)

We have investigated the passive transport of polymers and nano-particles through lipid membranes. This is motivated by the fact that some proteins and protein sequences such as TAT (cell-penetrating transactivator of transcription) and homeoproteins are capable of translocating across biological membranes and to enable cargo translocation into the cell interior. This is apparently independent of active biological processes of the living cell, but the physical mechanism behind has not yet been revealed. That the balance between hydrophobic and hydrophilic units is very important for membrane-active proteins is known since a long time. It has been shown in previous studies, that copolymers composed of short lipids can display translocation in various cells depending on the overall hydrophobicity of the copolymers.

Diffusive transport through cell membranes is not only a possible pathway to deliver cargo to the cell without the need of biological active and metabolic processes but provides insight into physical aspects of pore-formation and the evolution and function of trans-membrane proteins. Driven in particular by the last aspect we have considered a universal model of a lipid membrane implemented by a lattice-based Monte Carlo method (the so-called bond fluctuation model, BFM) which is a most efficient simulation tool for flexible molecules and polymers such as lipids and flexible proteins. Moreover, solvent and soft nano-particles can be simulated using this method. We have applied an explicit solvent model in order to avoid artifacts due to strong hydrophobic attraction, but also in order to study the permeability of the solvent through the membrane. A snapshot of the simulation box is shown in Fig. 1.

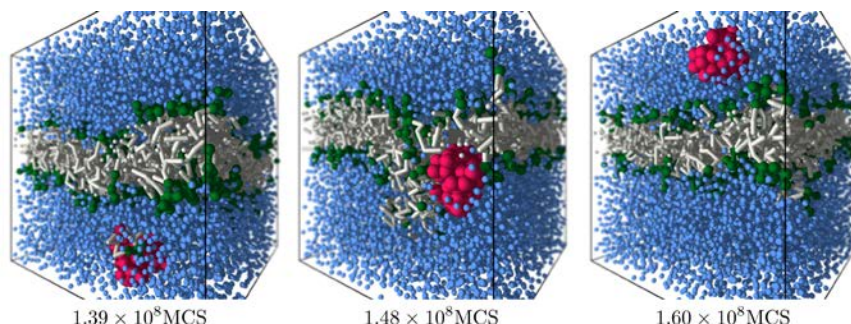


Fig. 1: Snapshots of a lipid bilayer membrane interacting with a homopolymer of balanced hydrophobicity. A translocation event can be directly observed.

During the project period we have investigated the following aspects of passive transport through lipid bilayer membranes:

- Homopolymers composed of monomers with varying degree of hydrophobicity: The role of balanced hydrophobicity.^{1,2}
- Nanoparticles with different degrees of hydrophobicity.³
- Copolymers consisting of hydrophilic and hydrophobic units: The role of sequence-length and optimal sequence analysis.^{4,5}

We found that homopolymers tend to adsorb on lipid membranes with increasing hydrophobicity of their monomers. A critical hydrophobicity leads to strong perturbation of the membrane in the environment of the polymer, see Fig.1 middle part, which leads to enhanced flip-flop dynamics of the lipids, enhanced permeability and eventually translocation of the polymer itself.^{1,2}

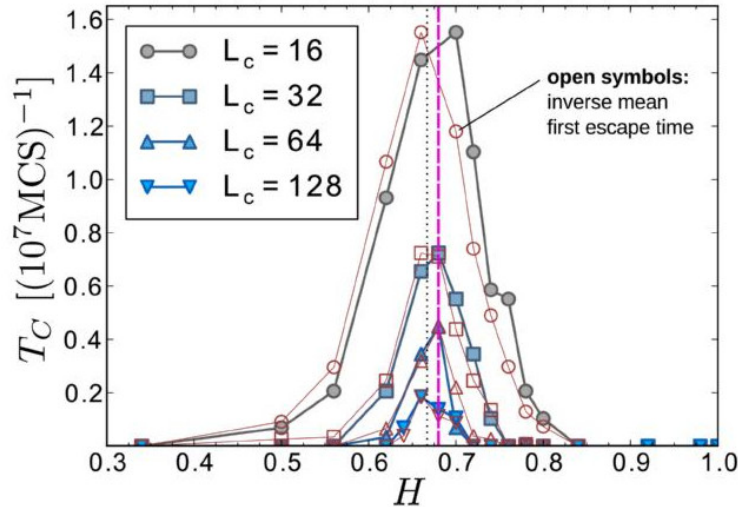


Fig. 2: Translocation rate vs. relative hydrophobicity of the homopolymer. Values of $H=0$ and $H=1$ corresponds to hydrophilic and hydrophobic monomers respectively. A maximum is displayed for $H=0.68$ for all chain lengths L_c . The results of the simulation (full symbols) are in excellent agreement with calculations using the free energy potential of the membrane with respect to the polymers chain (open symbols).

In Fig. 2 we show rate of translocations of the homopolymer as a function of the hydrophobicity of the monomers. Translocation can only be achieved at balanced hydrophobicity where the monomers segregate both from water and from the lipid. As a consequence translocation from the water to the lipid-phase is related with a weak potential barrier only. Since our model-membranes does not have biologically active functions this corresponds to a pathway of passive transport of the polymer. In analytical work, which has involved two Bachelor-thesis, we have analyzed the adsorption transition of the polymer based on a potential model of the lipid-bilayer and analyzed the critical adsorption properties. These studies reveal the role of a balanced hydrophobicity of the polymer as a key to maximize the perturbation of the membrane.

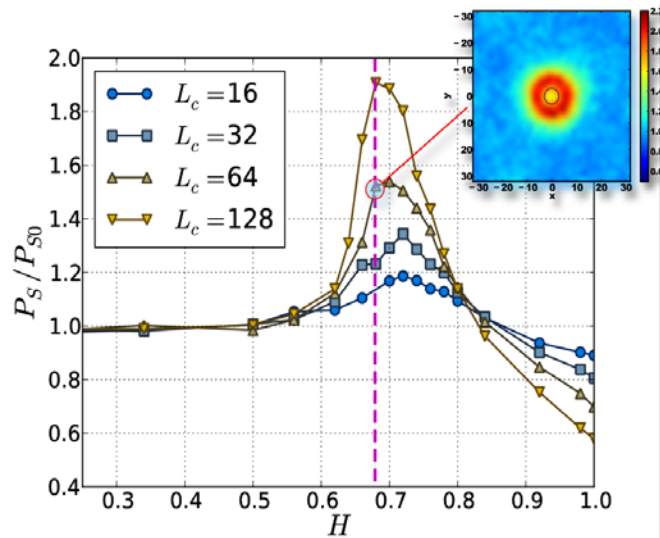


Fig. 3: Permeability of the solvent as a function of the hydrophobicity, H , of the polymer chain and for various chain lengths, L_c . At balanced conditions for about $H=0.68$ a maximum of translocations rate can be found. This maximum corresponds to the maximum of the translocation rate of the chain. The inset shows the local distribution of the permeability on the membrane surface around the location of the center of mass of the chain. A ring-like pore around the COM of the chain is carrying the highest permeability.

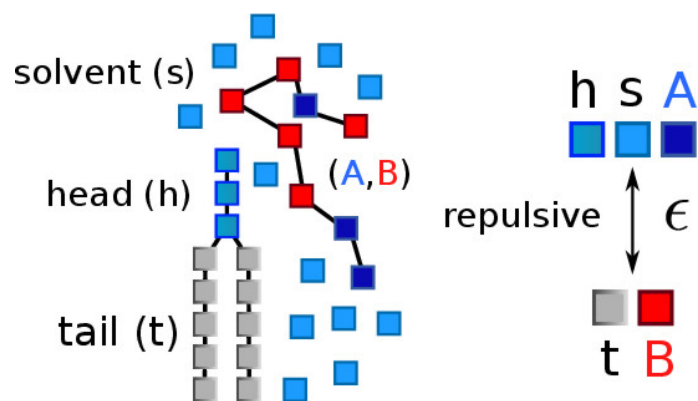


Fig. 4: Interaction model for copolymers, lipids and solvent. In the simplest case, solvent (water, s), head-groups (h) and A-type monomers (A) have the same interaction properties (fully hydrophilic). Tails (t) and B-type monomers (B) are fully hydrophobic. Thus a single microscopic interaction parameter (ϵ) is sufficient.

Another interesting aspect of these studies is the enhanced permeability of the membrane in the immediate environment of the adsorbed polymer with respect to the solvent. In Fig. 3 we show the relative permeability of the membrane as a function of the hydrophobicity of the chain. Coinciding with the adsorption threshold and the maximum of translocation of the chain, the permeability displays a maximum. The adsorbed chain at balanced hydrophobicity creates a pore for solvent permeation which can be shown to be related with an enhanced flip-flop rate of the lipids near the polymer chain. The shape of the pore is that of a hollow-cylinder, the center of mass of the chain rather blocking solvent permeability.

We have extended our work to copolymers where individual monomer units can carry a different hydrophobicity. This corresponds more closely to the case of (disordered) proteins as for instance nucleoporins. The interaction model is sketched in Fig. 4. Balanced hydrophobicity is now reached by an appropriate combination of hydrophilic (A-type) and hydrophobic (B-type) sequences. In addition to the case of homopolymers where each monomer has a balanced hydrophobicity, for copolymers the individual sequences of hydrophilic and hydrophobic units plays a role: longer sequences (higher blockiness) enhance localization of the copolymer instead of translocation. At balanced hydrophobicity, shorter sequences lead to higher translocation rates.

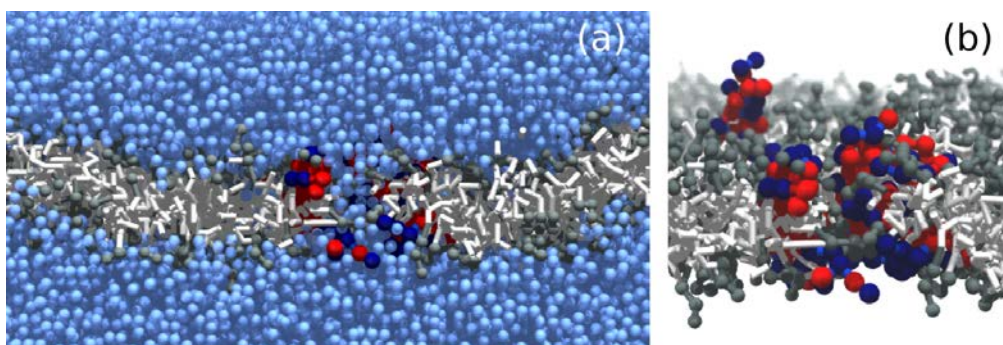


Fig. 5: Simulation snapshot of a random copolymer inserted across the membrane and inducing a transient pore. Lipid heads (h) are dark gray, lipid tails (t) are light gray, A-type monomers are dark blue, B-type monomers are red, solvent monomers (s) are light blue. (a) and (b) show the same configuration with solvent (a) and without solvent (b).

Also copolymers with a balanced distribution of hydrophobic and hydrophilic units cause an increased permeability with the respect to the solvent. We found *transient pore formation* by the random copolymer as displayed by the snapshots in Fig. 5. This may serve as a primitive model for the function of channel proteins in an early stage of evolution where secondary structure of proteins is not necessary. In a later stage of evolution the selection of specific sequences could have taken place to refine the function of pores.

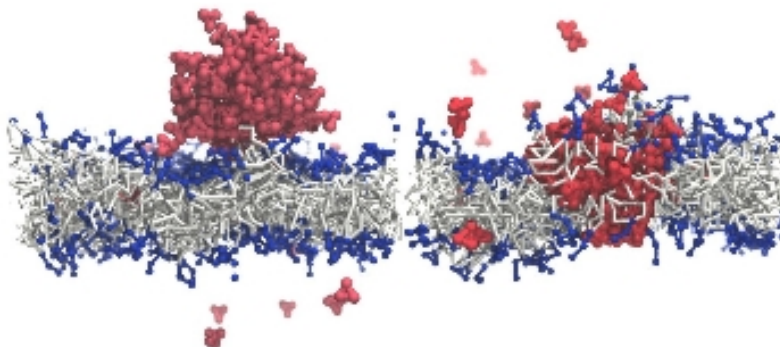


Fig. 6: Aggregate of amphiphilic nanoparticles interacting with a lipid bilayer before and after internalization into the membrane core.

We have also investigated the interaction of amphiphilic nanoparticles with model membranes.³ Similar to the case of homopolymers and copolymers, nanoparticles can be translocated through the membrane if a critical balance of hydrophobic and hydrophilic sites is reached. A snapshot of nanoparticles interacting with the lipid membrane is displayed in Fig. 6.

For homogeneous nanoparticles droplet formation in the pure phases, most noticeable in the aqueous phase, takes place, see Fig. 6. Using nanoparticles with a Janus-like structure composed of both hydrophilic and hydrophobic components can avoid droplet-formation by keeping the ability of translocation. This could be a strategy to synthesize nanoparticles which are not segregating in water but still can be hydrophobic enough to display internalization by the lipid-phase and translocation.

In summary, our studies have revealed the key role of balanced hydrophobicity of polymers and nanoparticles for passive transport as well as for the formation of pores during the attachment of these nano-objects. Passive transport of nano-objects such as proteins, DNA and nanoparticles can be a versatile method to influence cell function such as reprogramming cells or to achieve apoptosis for selected cells. Hydrophobically balanced copolymers may serve a cell-penetrating peptides either by combining with a cargo (to reached balanced conditions for the combined object) or to create transient pores which enable the translocation of the cargo-objects. Still it is not clear which particular mechanism is operating for typical cell-penetrating peptides to enable translocation even of relatively large objects (with the possibility of biologically active processes such as endocytosis) but our studies within this project revealed general physical mechanisms based on passive translocation pathways which can be explored in the future by experimental studies.

Engineering of CPP-fused proteins with intrinsic fluorescence labels and anchor groups (work group of Dr. Y. Zhang, TU Dresden)

Towards the goals of the project we have designed and synthesized two types of CPP-fused biologicals, including protein and oligonucleotides, and studied the interaction between CPP with artificial vesicles (GUV). These structures are based on CPP sequences reported in literature as well as on the results theoretical modeling reported above. Moreover, we have also investigated molecule/membrane interaction using other chemical groups such as lipid chain and cholesterol.

We have found that the conjugation between CPP and biologicals and the resulting effects on cell permeability do not exhibit a simple correlation. For example, when a CPP is conjugated to morpholinos, an ideal DNA analogue resistant to nucleases, no enhanced transfection can be achieved. In contrast, surprisingly, when the CPP is conjugated to DNA plasmid, an enhanced penetration can be achieved. Moreover, the resulting conjugate can cross the blood brain barrier as the compound was injected into zebrafish brain.

Furthermore, we have designed a complex conjugation system, containing a polymer-conjugated heparin binding peptide, and/or cell adhesion sequence, protease cleavable sequence, biotin, fluorescently labeled streptavidin. The resulting conjugate can interact with heparin containing polymer matrix, induce cell adhesion, be degraded with protease MMP produced by cells, and introduce other bio-functionality through biotin-streptavidin interaction. The conjugation system is synthesized using various types of orthogonal chemical reactions.

Besides, we have designed a repertoire of peptide tags, whose release can be controlled through the interaction (binding and dissociation) with oligosaccharides. The peptides are conjugated with either drug compound such as immunosuppressive drug cyclosporin A or fluorescent compound such as fluorescein. Most importantly, through this study, we have discovered a tag (ATIII), which can be released from the polymer matrix through a zero order process. We are now conjugating this tag to FGF and VEGF, to generate a sustainable morphogen releasing system.

Development of cell-penetrating cargo (work group of Dr. Y. Zhang, TU Dresden)

DNA origami became a powerful tool for creating custom-shaped functional biomolecules. We reported the first approach towards assembling amphipathic three-dimensional DNA origami nanostructures and assessing their dynamics on the surface of freestanding phospholipid membranes. Our nanostructures were stiff DNA origami rods comprising six DNA helices. They were functionalized with hydrophobic cholesteryl-ethylene glycol anchors and fluorescently labeled at defined positions. Having these tools in hand, we could demonstrate not only the capability of the amphipathic nanorods to coat membranes of various phospholipid compositions, but also their switchable liquid-ordered/liquid-disordered partitioning on phase separated membranes. The observed translocation of our nanostructures between different domains was controlled by divalent ions. Moreover, selective fluorescent labeling enabled us to distinguish between the translational and rotational diffusion of our six-helix bundles on the membranes by fluorescence correlation spectroscopy. The obtained data reveal how DNA origami can be employed as a valuable tool in membrane biophysics.⁶

Using biotinylated CPP in combination with fluorescently labeled streptavidin protein we have established a method, not only to identify potent CPP to assist protein cargo to penetrate cell membranes, but also to discover the optimal combination of them on one cargo protein, which would maximize the protein delivery. With this strategy, we mainly intended to combine screening and rational design approaches.

As an example, we have collaboratively explored CPP transfer into brain tissue. Zebrafish brain can regenerate lost neurons upon neurogenic activity of the radial glial progenitor cells (RGCs) that reside at the ventricular region. Understanding the molecular events underlying this ability is of utmost interest for translational studies of regenerative medicine.

Therefore, functional analyses of gene function in RGCs and neurons are essential. Using cerebroventricular microinjection (CVMI) RGCs can be targeted efficiently but the penetration capacity of the molecules injected, reduce dramatically in deeper parts of the brain tissue such as the parenchymal regions that contain the neurons. We identify a short cell-penetrating peptide (CPP), which can robustly penetrate the brain tissue without any overt toxicity.

Cargo molecules that are attached to the peptide can also be carried along in a size-dependent manner and this serves as a rapid tool for delivery into brain tissue. Combined with the advantages of cerebroventricular injection method such as rapidness, reproducibility, and ability to be used in adult animals, CPPs improve the applicability of the CVMI technique to deeper parts of the tissues not only in the central nervous system but also in various other organs.⁷

Development and characterization of ultra-thin (UT) starPEG-Heparin hydrogel matrices (work group of Prof. C. Werner, IPF)

In order to achieve the goals of using a starPEG-heparin hydrogel for delivering CPPs to cells in the production of iPS cells, ultra-thin films (< 200nm) of starPEG-heparin hydrogels were prepared and characterized using atomic force microscopy and confocal laser scanning microscopy (CLSM). The films retained the same mechanical properties, as evaluated via the Young's moduli, and swelling behavior as their bulk counterparts.

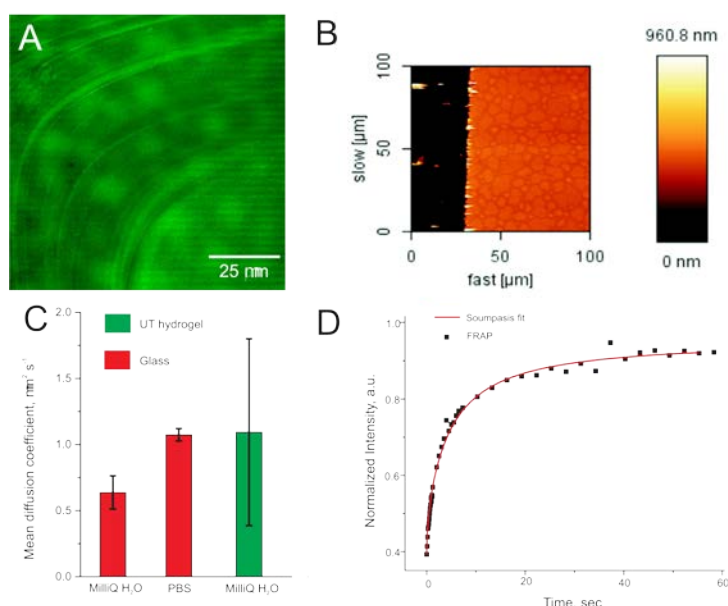


Fig. 7: (A) CLSM image of a SLB of DOPC-NBD-PC 0.5 mol% on an UT hydrogel films. Note the slightly higher intensity circular regions. (B) These features coincide with AFM images obtained of similar swollen UT hydrogel films. (C) Mean diffusion coefficients of DOPC-NBD-PC 0.5 mol% SLBs on an UT hydrogel film (green) and plasma cleaned glass (red) in MilliQ water and PBS, as measured by FRAP. Statistically, there is no difference between the mean diffusion coefficient on glass in PBS and the UT hydrogel film in MilliQ water. However, there is a clear difference in the variation. The differences in the mean diffusion coefficients on glass in MilliQ water and on UT hydrogel in MilliQ water are significant ($p = 0.0059$). (D) A typical FRAP curve obtained for a SLB of DOPC-NBD-PC 0.5 mol% on an UT hydrogel film depicted in (A). From Ref. 8.

We further characterized the properties of these hydrogel films interacting them with supported lipid bilayers (SLBs) and giant unilamellar vesicles (GUVs). Fig. 7 shows representative results of planar lipid bilayers on UT hydrogel films and shows comparison with glass substrates. The diffusion of the lipids in the bilayer was evaluated using the fluorescence recovery after photobleaching (FRAP) technique. The results suggest a larger variation in the diffusion coefficients of lipids within the lipid bilayer on UT hydrogel films compared to glass.⁸ We conclude that this is related to the non-homogeneous structure of the UT hydrogel (Fig. 7A & B).

Development of non-covalent bio-matrices (work group of Dr. Y. Zhang, TU Dresden)

Formation of hydrogels by receptor-ligand interactions

As an alternative type of gel matrix for supporting CPP delivery, we have developed a novel, non-covalent hydrogel system crosslinked solely by receptor-ligand interactions between biotin and avidin. The simple hydrogel synthesis and functionalization together with the widespread use of biotinylated ligands in biosciences make this versatile system suitable for various applications. The gels possess a range of tunable physical properties, including stiffness, lifetime and swelling. Unexpectedly fast hydrogel erosion provides new insight into force loading-rate dependent receptor-ligand interactions in supramolecular networks, previously only studied at the single molecule level. Physical calculations were used to rationalize the gel's strict concentration dependent formation, as well as the erosion rates. As a proof of utility, the gels were functionalized with different peptide sequences and applied to control human mesenchymal stromal cell morphology in 3D culture.^{9,10}

Minimal peptide motifs for non-covalent hydrogel formation

Reduction of complexity of the extracellular matrix (ECM) to a non-covalent structure with minimal chemically defined components represents an attractive avenue for understanding the biology of the ECM. The resulting system could lead to the design of tailor-made biomaterials that incorporate varying functionalities. Negatively charged glycosaminoglycans are the major components of the ECM. Their interaction with positively charged proteins is important for dynamic three-dimensional scaffold formation and function. We designed and screened minimal peptide motifs whose conjugates with polyethylene glycol interact with heparin to form non-covalent hydrogels. Here we show the structure/function relationship of the (RA)_n and (KA)_n motifs and determined that both basic residues and the heparin-induced α -helix formation are important for the assembly process. Simple rules allowed us to tune various aspects of the matrix system such as the gelation rates, biodegradability, rheological properties, and biofunctionality. The hydrogels can encapsulate cells and support cell survival.¹¹⁻¹³

Conjugable tags

A repertoire of conjugable tags for controlling the release of drugs from biomaterials is highly interesting for the development of combinatorial drug administration techniques. We developed such a system of 11 peptide tags derived from our previous work on a physical hydrogel system cross-linked through peptide-heparin interactions. The release kinetics of the tags correlate well with their affinity to heparin and obey Fick's second law of diffusion, with the exception of the ATIII peptide, which displays a stable release profile close to a zero-order reaction. A system for release experiments over seven months was built, using the hydrogel matrix as a barrier between the reservoirs of tagged compounds and supernatant. The gel matrix can be injected without affecting the releasing properties. A tagged cyclosporin A derivative was also tested, and its release was monitored by measuring its biological activity. This work represents a design of biomaterials with an integral system of drug delivery, where both the assembly process of the matrix and affinity capture/release of tagged compounds are based on the noncovalent interaction of heparin with one class of peptides.¹⁵

Matrix-metalloproteinase and photosensitive peptide units

Matrix-metalloproteinase and photosensitive peptide units were combined with heparin and poly(ethylene glycol) into a light-sensitive multicomponent hydrogel material. Localized photo-degradation of the hydrogel matrix allows the creation of defined spatial constraints and adhesive patterning for cells grown in culture. Using this matrix system, it was demonstrated that the hydrogel structure determines the fate of neural precursor cells *in vitro*. The most interest outcome in this study was the observation that the multi-functionally patterned matrix can provide a versatile and tunable system to model a neurogenic niche, not only through orchestrating the extracellular and intracellular signaling, but also by tuning the various physical parameters such as degree of confinement.

Cell growth on flat surfaces, in channels, or in holes could represent spatial confinement in zero, one, or two dimensions, respectively, when the scale of the channels or holes are comparable to the size of cells.¹⁶

Layer-by-layer assembly of hydrogel matrices

Bioengineering utilizing the principles of self-assembly holds many promises towards nanotechnology based applications in biotechnology and material sciences. Glycosaminoglycans like heparin are important constituents of the extracellular matrix. Semi-synthetic heparin based hydrogels, formed with the help of multi-arm or star shaped polyethylene glycol (starPEG) have been instrumental towards range a of environment-function-relationship studies. A screen of heparin binding peptides yielded very strong binders. Coupling the peptides to starPEG enabled the formation of hydrogels in bulk and controlled layer-by-layer assembly yielded ultra-thin bio-layers in the nanometer range that supported cell culture. The ultra-thin layers could be patterned and the build-up the layer was characterized using quartz crystalline microbalance and imaged using atomic force microscopy. The microscopy in situ revealed a defined change in morphology. We can place a bioactive layer in the layer-by-layer structure with nanometer precision, and detect the remarkable different in their interaction with cells. This work illustrates how biochemical and physical cues affect cell fate synergistically.

High-throughput translocation assay for screening CPP designs (work group of Prof. C. Werner, IPF)

A high-throughput assay for screening membrane translocation of fluorescently labeled CPPs and CPP-TF constructs was developed using GUVs and fluorescence activated cell sorting (FACS). The detection principle of this assay is based upon the shift of the fluorescence intensity signal when the CPP is exposed to a different pH value inside the GUVs. In order to determine if the peptides were translocating and entering the lumen of the GUVs, we established a FACS experiment where all CPPs associated with the lipid membrane are quenched using DOPE-ATTO 540Q, and the intensity of the CPP fluorescence is dependent upon the internal pH of the GUV. Therefore, GUVs were prepared with a internal pH value of 7 and 4 and both with and without the fluorescence quencher DOPE-ATTO 540Q. Our results clearly indicate the translocation of CPPs, such as Transportan (Trans) and the transactivator of transcription (TAT) peptide, as seen in Fig. 8. All FACS results were correlated to CLSM images of GUVs.

In addition to simple, single lipid GUVs, we investigated more complex lipid mixtures as cell models. We developed a lipid mixture to mimic the lipid membrane of a human fibroblast cell, containing 5 different lipid types. Using this mixture, we produced so-called "fibroblast GUVs" for our FACS assay and CLSM. We found that the more complex mixture produced an improved translocation of CPPs. These data suggested that an even better model might be to derive lipid membranes directly from cells. Therefore, we optimized a protocol to produce giant membrane plasma vesicles from mouse fibroblast cells and studied their uptake of CPPs using CLSM and FACS (Fig. 9). However, as we would be unable to modulate the internal pH of the giant membrane plasma vesicles, we developed an alternative method for determining translocation, using FRET between the CPP dye, Atto-488, and TagRFP, which was expressed in the cytosol by transfected cells.

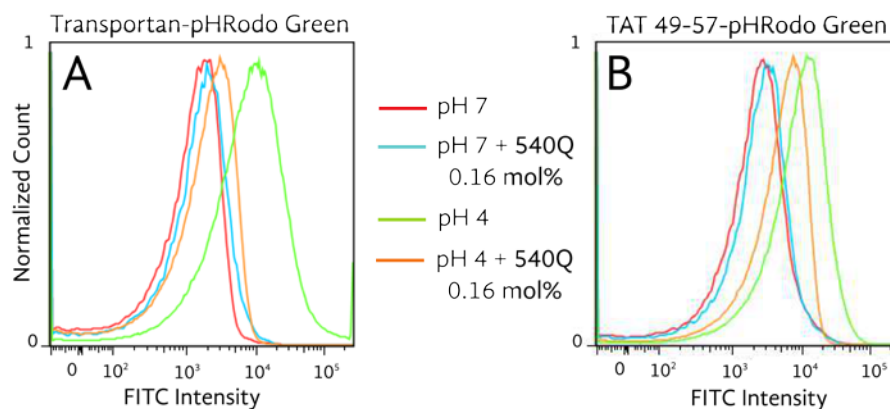


Fig. 8: FACS histograms of DOPC GUVs incubated with Transportan (A) and TAT 49-57 (B) peptides linked to the pHrodo® fluorophore. There are two types of labeled GUVs, those with and without the fluorescence quencher DOPE-ATTO 540Q ("540Q"), which quenches the emission of the pHrodo dye when it is associated with the lipid membrane. In addition, the internal pH in the GUVs is different, pH 7 and pH 4. The fluorescence emission intensity of the pHrodo dye is low at pH 7 and high at pH 4.

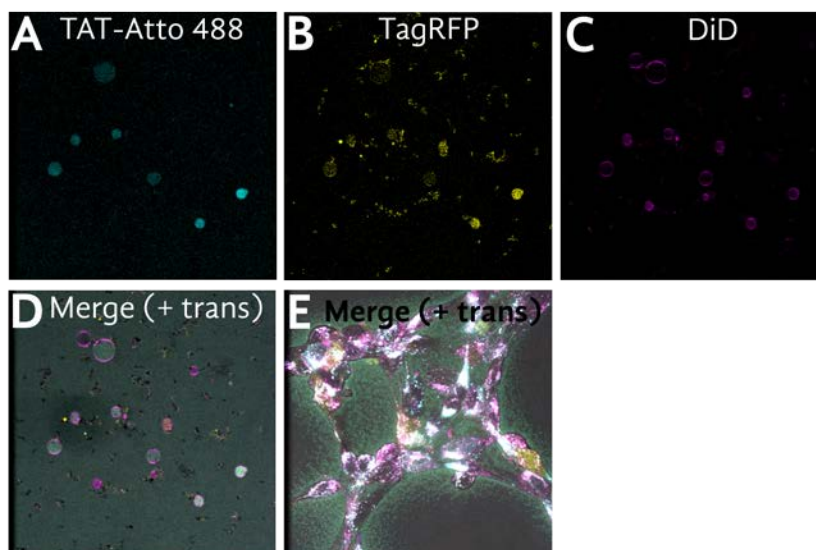


Fig. 9: CLSM images of giant plasma membrane vesicles incubated with 2 μ M TAT 49-57 peptide (RKKRRQRRR) labeled with Atto 488 dye. The vesicles were obtained from transfected NIH/3T3 cells with cytosolic expression of TagRFP. The fluorescence emission of Atto-488 was used to excite the TagRFP and hence, is a reporter of cytosolic delivery of CPPs to the cells/vesicles. The lipid membranes of both the cells and giant plasma membrane vesicles were stained with DiD. Panels A, B, C & D are the TAT-Atto-488, TagRFP, DiD (lipid membrane), and merge (including transmembrane) channels, respectively, for giant plasma membrane vesicles. Panel E uses the same color coding as panels (A-D) in NIH/3T3 cells to demonstrate that the TAT 49-57 peptide appears to be co-localized with the TagRFP in the cytoplasm *in vivo*. Each image is 145 x 145 μ m.

Adhesion between model cells and UT hydrogel films for CPP delivery (work group of Prof. C. Werner, IPF)

It is important to study the interactions of the GUVs with the hydrogel system, both in the presence and absence of the CPPs. Hence, using GUVs as model cell membranes, we measured the effective contact angles of GUVs on ultra-thin (UT) starPEG-heparin hydrogel films and glass using confocal laser scanning microscopy (CLSM). From our images, we calculated estimates of the membrane lateral tension and the specific adhesion energies of the GUVs. Despite differences in the average contact angles of GUVs on UT hydrogel films versus glass, we found that the lateral membrane tensions were approximately constant and vesicles on both substrates remained in the gravity-induced adhesion regime.¹⁴ However, when UT hydrogel films were pre-loaded with the CPP Transportan or vesicles were exposed to Transportan on glass, there was a transition from gravity-induced adhesion to the strong adhesion regime.¹⁴ In contrast, the CPPs poly(arginine) (Poly R) and Antennapedia peptide (AntP) did not show a change in contact angle or adhesion energy. In summary, these results suggest that delivery of CPP-transcription factor conjugates into cells, using starPEG-heparin hydrogel ultra-thin films, may have effects on the specific adhesion energy of the cells with the substrate. Hence, further studies of the impact that the CPP-hydrogel system has on cells, including possible cytotoxic effects, using different material combinations are required.

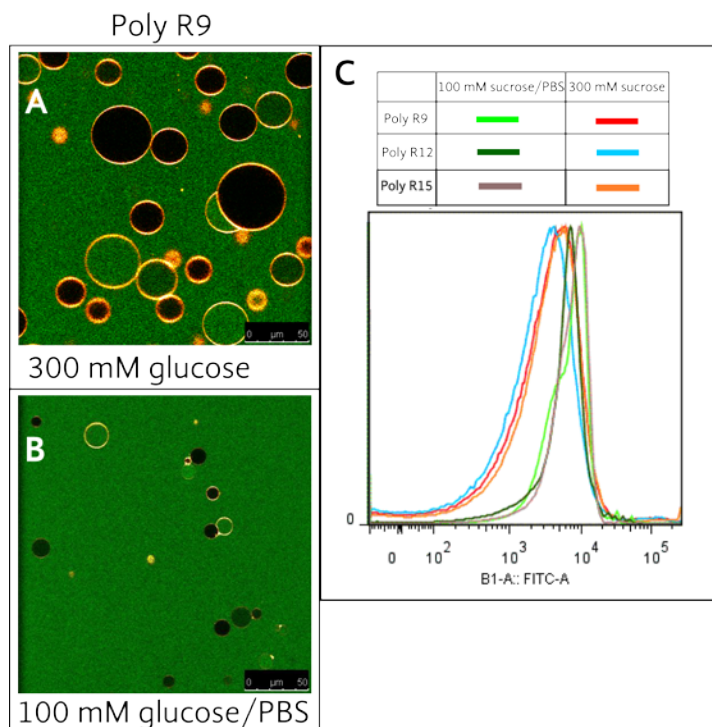


Fig. 10: CLSM images of DOPC GUVs observed in 300 mM glucose solution (A) and in 100 mM glucose/PBS solution (B) with 10 μ M Poly R9 (A & B). GUVs were prepared in 300 mM sucrose for imaging in 300 mM glucose and in 100 mM sucrose/PBS for imaging in 100 mM glucose/PBS. (C) FACS histograms of GUVs that were incubated for 1 hour with 4 μ M Poly R9 (RRRRRRRRR), Poly R12 (RRRRRRRRRRRR) and Poly R15 (RRRRRRRRRRRRRRR) peptide solutions. The GUVs were grown in 300 mM sucrose or 100 mM sucrose/PBS. In all cases, the samples were analyzed using the running buffer of the FACS machine, which contained PBS.

Improving delivery via CPP-anion interactions (work group of Prof. C. Werner, IPF)

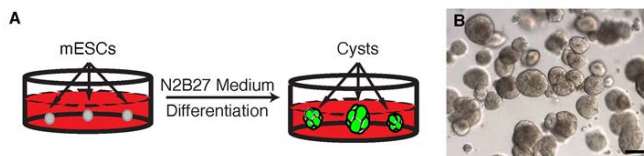
Recently, there has been evidence that certain co-anions, such as phosphates in PBS or pyrene butyrate, complex with highly charged poly arginine or TAT peptides¹⁷⁻¹⁹, allowing them to pass through lipid membranes. It is believed that this effect is related to the guanidinium cations present in poly(arginine) and TAT. Hence, this effect is specific to peptides containing arginine. We investigated the translocation of different lengths of poly(arginine) with GUVs using CLSM (Fig. 10A & B) and FACS (Fig. 10C). We found that when DOPC vesicles were produced in sucrose solution only and then were incubated with various length poly(arginine) peptides, the translocation ratio was lower than when the vesicles were produced in sucrose/PBS solution. The underlying mechanisms are currently studied at immobilized poly(arginine) layers in various buffers with the co-anions phosphate and pyrene butyrate using microslit electrokinetic experiments.

Novel CPPs based upon computer simulations (work group of Prof. C. Werner, IPF)

Finally, we investigated new designs of peptides based upon results of computer simulations from the group of Prof. Jens-Uwe Sommer. Using Monte Carlo simulations, it was found that the translocation rate of AB block copolymers, where one block was hydrophobic and the other was hydrophilic, was increased when the hydrophobic block was tailored to be a particular percentage of the thickness of the lipid membrane (see also results above). Using these results, the group of Y. Zhang synthesized a series of peptides consisting of arginine and alanine, Poly RA, Poly RAA and Poly RAAA, where the total number of amino acids was kept constant and therefore the size of the hydrophobic sections of the peptides was varied. Based upon the computer simulations, the Poly RA peptide should have the correct length for a DOPC membrane to demonstrate enhanced translocation compared to the other peptides. We found that at all concentrations investigated, the Poly RA peptides exhibits a higher translocation.²⁰

Differentiation of iPS cells triggered by multifunctional natural and bioengineered matrices (work group of Prof. E. Tanaka, MPI-CBG Dresden)

The Tanaka laboratory explored the end phase of the aims - the culturing of cells in a condition compatible with propagating the pluripotent state and differentiation of the pluripotent state in three dimensional conditions, both using natural and bioengineered matrices. Toward the latter aim we used both mouse and human embryonic stem cells as the starting point for exploring the three dimensional differentiation conditions of pluripotent stem cells to the neural lineage.²¹⁻²⁵ The aim of these studies was to reconstitute complex neural tissues that would have functional consequences including as a source for potential in vivo transplantation.



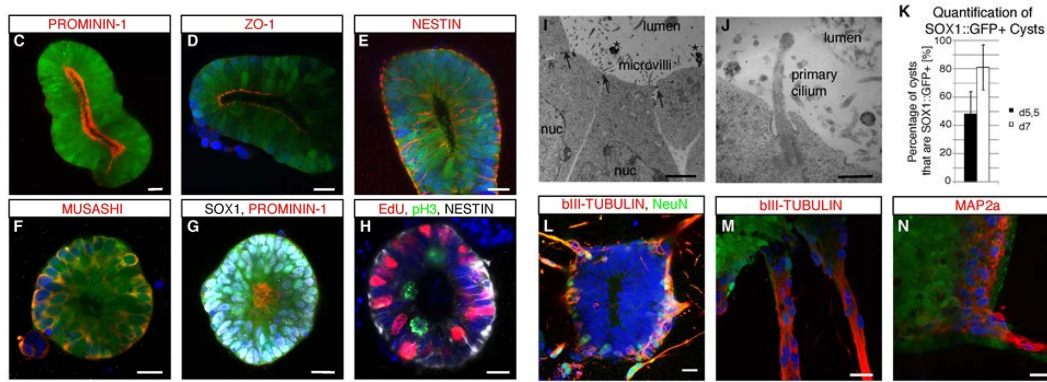


Fig. 11: Characterization of neural cysts derived from mESCs. All data shown here were derived with the SOX1::GFP reporter cell line 46C. All immunofluorescence panels (C-H, L-N) represent confocal images of 3D cysts. (A) Scheme of the generation of neural cysts. Within 5 days neuroepithelial cysts form that express SOX1::GFP and possess a single lumen (B). Day 6 neural cysts are apicobasally polarized as shown by the luminal expression of PROMININ-1 (C, G) and the tight junction marker ZO-1 (D). The neural stem cell markers NESTIN (E) and MUSASHI (F) are also being expressed. To show that SOX1::GFP cysts are 100% neural in character we also stained for the protein SOX1 (white nuclei, G). (H) Cells in a cyst undergo interkinetic nuclear migration as evidenced by staining for phosphorylated Histone 3 and the thymidine analogue EdU. Cells undergoing division are located at the apical side (pH3⁺) whereas cells in S-phase which are EdU⁺ are located at the basal side. (I, J) Electron microscopic analysis of early neuroepithelial cysts. Cysts possess tight junctions (arrows), have large apical membrane surfaces with microvilli and primary cilia (J) and shed midbodies (stars) into the lumen. (K) Quantification of SOX1::GFP⁺ cysts at day 5,5 and day 7 of differentiation. Data are represented as mean ± SD. (L-N) Around d7-d8 postmitotic neurons start to grow out basally as evidenced by NeuN (L) and βIII-TUBULIN (L, M) as well as MAP2a (N). Nuclei were counterstained with Hoechst. Scale 20 μm (C-H, L-N); 2 μm (I), 0,5μm (J).

Three dimensional mouse ES cultures that self-pattern the spinal cord

Working with mouse ES cells, we sought to differentiate pluripotent cells into three dimensional spinal cord. Starting with the natural matrix, Matrigel, combined with neural induction conditions, we found that single cell suspensions of mouse ES cells would efficiently and clonally form neuroepithelial containing a single lumen, resembling the embryonic neural tube, structures that we call neural cysts. Remarkably, the cells progressed as if through normal development, first expressing markers of primitive ectoderm before turning on neural markers. The neural cysts displayed interkinetic nuclear migration, and by 14 days progressed to generate differentiated neurons at the outer circumference of the organoids, as is observed in normal embryonic development (Fig. 11).

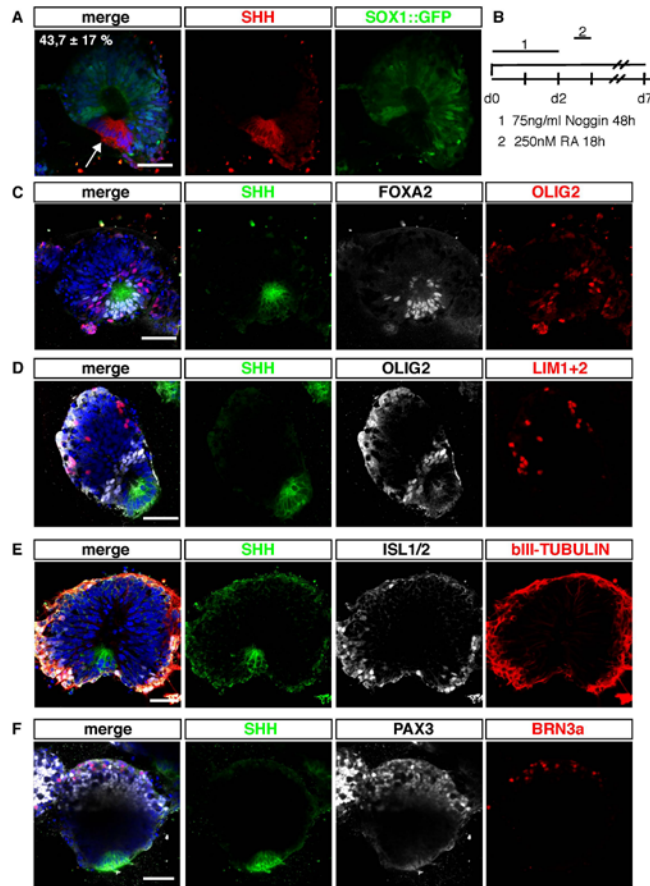


Fig. 12: Self-organized DV patterning in posteriorized neuroepithelial cysts. (A) Self-patterned neuroepithelial cysts derived from 46C ESCs show that the FP region which is SHH⁺ (red) is SOX1::GFP⁻ and has basally localized nuclei (arrow). (B) Scheme of the experimental setup. (C) The FP region co-expresses SHH (green) and FOXA2 (white). Close to the FP region but not directly adjacent to it the progenitor marker OLIG2 (red) stains on both sides, corresponding to the pMN region. (D) The FP is marked by SHH expression (green) and the pMN region in white by OLIG2 expression. Further dorsal the interneuronal marker LIM1+2 (red) can be detected. (E) MNs identified by ISL1/2 stainings (white) can be detected close to the FP region stained with SHH (green) as well as dorsally. β III-TUBULIN immunostaining (red) shows peripheral arrangement of differentiated neurons and their axons. (F) PAX3 (white) as a general dorsal marker and BRN3a (red) as a differentiation marker for dorsal interneurons were the furthest dorsal markers detected in self-patterned cysts. The FP region is marked in green by SHH. All nuclei were counterstained with Hoechst. Scale 50 μ m.

However, this neural tissue was of dorsal brain identity. We sought to posteriorize the neural cysts via addition of retinoic acid, which when added early, 48 hours before cyst formation, posteriorized the cysts to cervical levels. In an unexpected result, this retinoic acid addition resulted in generation of a localized floorplate that expressed sonic hedgehog protein—the ventral-most signalling center within 50% of the cysts (Fig. 12). The presence of the signalling center combined with the natural expression of dorsal signalling factors in the cysts remarkably yielded patterning of the cysts to generate the different neuronal progenitor cell types ranging from ventral motor neurons to dorsal sensory interneurons. We further showed that the floorplate induction required active sonic hedgehog signalling (Fig. 13).

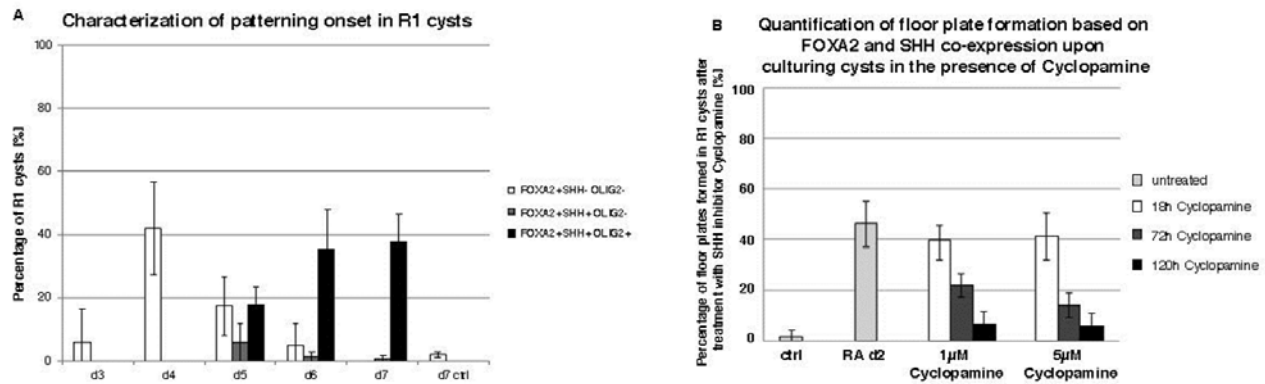


Fig. 13: Characterization of FP induction by RA. (A) Quantification of patterned cysts after stimulation with 100 nM, 250 nM and 750 nM RA for 9 hours, 18 hours and 24 hours. R1 cysts were analyzed on day 7 by immunostaining for SHH and OLIG2 and the percentage of cysts that were double-positive was determined. 9 hours of incubation with 100 nM RA lead to the formation of $7,2 \pm 3,3\%$ of self-patterned R1 cysts. This number increased significantly when the incubation period was prolonged to 18 hours ($28,3 \pm 7,6\%$) or 24 hours ($30 \pm 2\%$). The total fraction of patterned cervical cysts at 100 nM RA irrespective of incubation length never reached the same percentage as that obtained with 250 nM RA or 750 nM RA. Incubation with 250 nM RA or 750 nM RA lead to similar results at any timepoint investigated (9h incubation: $25 \pm 2,6\%$ at 250 nM RA; $27,1 \pm 5,4\%$ at 750 nM RA; 18 hours or 24 hours incubation: around 40% of patterned cysts). These results indicate that optimal cyst patterning is dependent on a certain RA concentration and incubation time. (B) Characterization of the patterning onset in R1 cysts. Day 4, day 5, day 6 and day 7 cysts were stained for OLIG2, FOXA2 and SHH after RA application on day 2 and the percentage of R1 cysts that was positive for any combination of the 3 markers, notably FOXA2⁺ SHH⁻ OLIG2⁻; FOXA2⁺ SHH⁺ OLIG2⁻ and FOXA2⁺ SHH⁺ OLIG2⁺, was determined. (C) Inhibition of FP induction through the administration of the SHH signaling inhibitor Cyclopamine. 1 µM and 5 µM Cyclopamine was added together with RA on day 2 for 18h, 72h or 120h to growing cysts. On day 7 the percentage of patterned cysts based on the co-expression of FOXA2 and SHH was determined. FP induction was almost completely inhibited when cysts were grown for 120 h in 1 µM or 5 µM Cyclopamine. Data are represented as mean \pm SD (n = 3).

Now that we had established a three dimensional system for neuroepithelial cyst formation, we next explored the minimal essential natural and bioengineered matrices that could support such patterned cyst formation. We found that patterned cysts could form in pure laminin-entactin gels as well as PEG hydrogels. Indicating that the cells themselves harbored all the information required to self-organize a cyst. Interestingly, this minimal cyst formation only occurred at relatively high densities of initial cell suspensions, and our preliminary results indicate that FGF5 and laminin can substitute for paracrine factors, allowing cyst formation in low cell density conditions (Ranga, Lutolf, Eberle preliminary results).

Human three-dimensional neuroepithelia recapitulate retina development and act as a homogeneous source of cells for transplantable retinal pigment epithelium

We next sought to generate equivalent cultures from human embryonic stem cells. The human cells differ from mouse cells in the difficulty of culturing from single cell suspensions, but we found that suspension of cell clusters in Matrigel efficiently resulted in neural cyst formation within 24 hours after initiating the culture (Fig. 14). In contrast the default identity of the cysts was not forebrain but rather retina. Several initial attempts to posteriorize cysts to cervical levels were not yet successful.

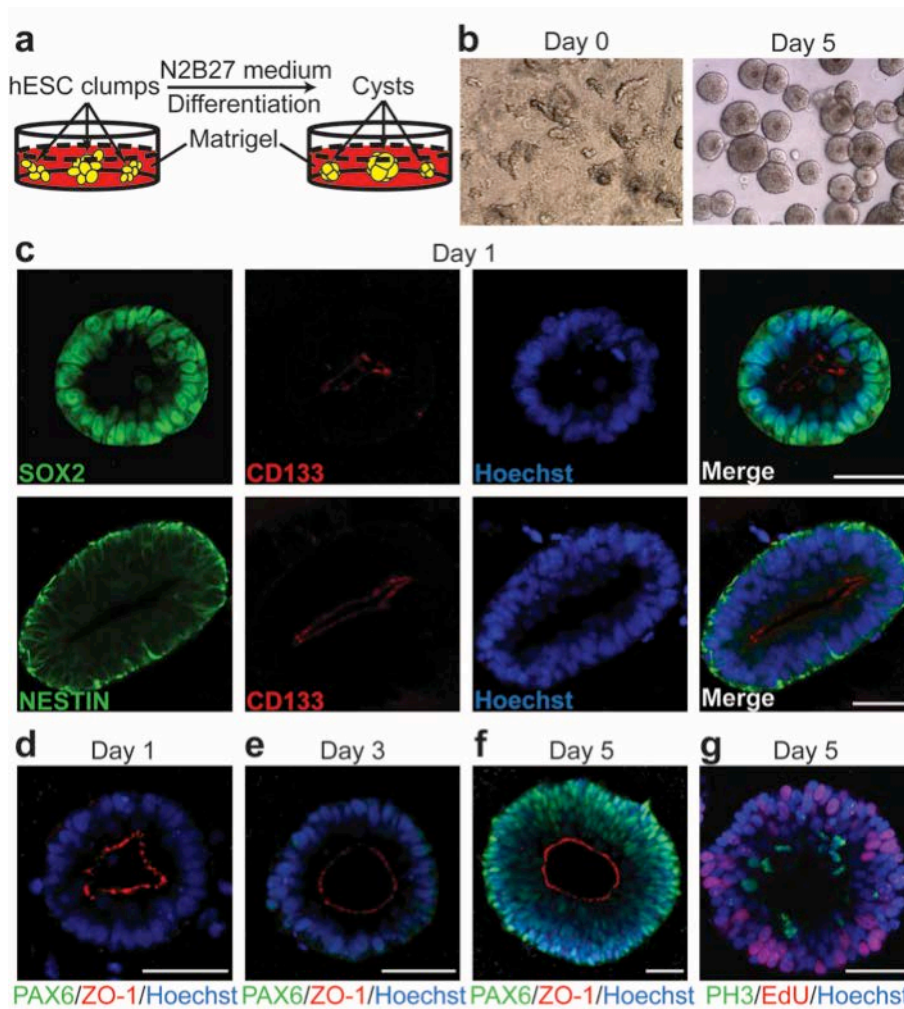


Fig. 14: Efficient generation of polarized neural progenitors from hESCs in a Matrigel-based 3D neuroepithelial cyst model. (A) Schematic of the experiment. (B) hESC clumps found at Day 0 formed neural tube-like cysts with a single lumen by Day 5. (C) By Day 1, hESC-derived cysts were positive for SOX2 and NESTIN. The apical localization of CD133 indicates apicobasal polarity is firmly established. (D) Immunostaining of PAX6 and ZO-1 during cyst growth in Matrigel. PAX6 was strongly expressed in Day 5 cysts that display clear properties of a pseudostratified epithelium. (E) M-phase cells stained with Phospho-Histone H3 (PH3) antibody only localized at the apical side of the cysts and S-phase cells labeled with EdU at the basolateral side, indicating that luminal mitosis occurred within the cysts. Nuclei were counterstained with Hoechst. Scale bar, 50 μ m.

Our institute has an interest in retinal tissue as a target tissue for regenerative therapies, including groups that work on preclinical models of cell transplantation to rescue retinal degeneration. Due to this environment, we chose to pursue the differentiation of the retinal cysts to differentiated cell types. To determine if the cysts had the potential differentiate into neural retina versus pigmented epithelium, we plated the cysts onto transwell filters under neural differentiation or Retinal Pigment Epithelium (RPE) differentiation conditions. We observed robust and complete differentiation to the two different cell types (Fig. 15), with the differentiation of the RPE being more complete and faster than any protocol previously described.

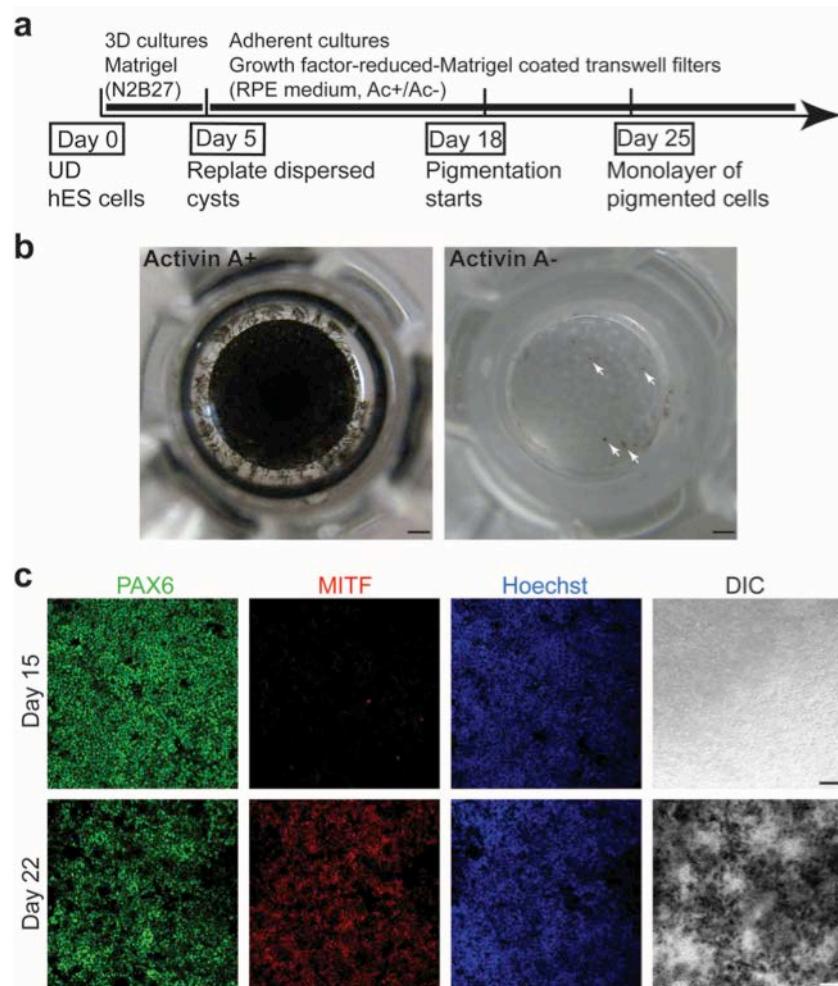


Fig. 15: Directed differentiation of hESC-derived cysts to RPE using transwell filters. (A) Schematic of RPE differentiation protocol. UD: undifferentiated. Ac+/Ac-: with or without Activin A. (B) Top view of transwell filters at 30 days of culture showing the appearance of a pigmented cell sheet in the presence of Activin A (100 ng/ml) but not its absence. Arrows (↘) point to a few pigmented foci in the non-Activin A treated sample. (C) Immunostaining of PAX6 and MITF at Day 15 and Day 22 during RPE differentiation. Expression of PAX6 remained stable, while MITF was up-regulated by Day 22. Scale bars, 1 mm (B), 50 μ m (C).

Transplantation of these RPE cells into two different models of RPE dysfunction yields engraftment and rescue of photoreceptor degeneration. Interestingly in the chemically induced model of RPE degeneration, the transplanted HESC derived RPE cells, when transplanted as a cell suspension form an intact, faithfully formed monolayer, a phenomenon not yet described in such transplantations.

In summary, we have generated culture conditions for pluripotent cells to form three dimensional neuroepithelia that faithfully reconstitutes several functions and traits of these tissues.

Summary

Aiming at the exploration of new therapeutic avenues for curing previously untreatable diseases by the application of induced pluripotent stem cells we applied a multidisciplinary research concept to identify new pathways and peptide structures for the delivery of cargo into cells. Towards this goal, we performed computer simulations to study translocation mechanisms of polymers and nano-particles through lipid bilayer membranes. Our studies have revealed the key role of balanced hydrophobicity of polymers and nanoparticles for passive transport as well as for the formation of pores during the attachment of these nano-objects. Based on the simulation results we identified and synthesized new peptide structures. To deliver these peptides into cells, we further synthesized and characterized different types of multibiofunctional hydrogel matrices. The translocation of these peptides into model systems (GUVs of various lipid composition and fibroblast-derived GUVs) was further studied in tailored screening assays. These experiments have shown that the interactions between the hydrogel, CPPs and cells may be modulated and likely leads to lower concentration levels in the therapeutic application of matrix-based delivery concepts. Finally, we cultured cells in a condition compatible with propagating the pluripotent state and differentiation of the pluripotent state in three dimensional conditions, both using natural and bioengineered matrices. For the latter aim, we used both mouse and human embryonic stem cells as the starting point for exploring the three dimensional differentiation conditions of pluripotent stem cells to the neural lineage. The aim of these studies was to reconstitute complex neural tissues that would have functional consequences including as a source for potential transplantation. With these experiments, we have identified culture conditions for pluripotent cells to form three dimensional neuroepithelia that faithfully reconstitute several functions and traits of these tissues.

References

1. J.-U. Sommer, M. Werner, V. Baulin, Critical adsorption controls translocation of polymer chains through lipid bilayers and permeation of solvent, *Europhys. Lett.*, 2012, 98, 18003.
2. M. Werner, J.-U. Sommer, V. Baulin, Homo-polymers with balanced hydrophobicity translocate through lipid bilayers and enhance local solvent permeability, *Soft Matter*, 2012, 8, 11714.
3. S. Pogodin, M. Werner, J.-U. Sommer, V. Baulin, Nanoparticle induced permeability of lipid membranes, *ACS Nano*, 2012, 6, 10555.
4. M. Werner, J.-U. Sommer, Translocation and induced permeability of random amphiphilic copolymers interacting with lipid bilayer membranes, *Biomacromol.*, 2014, submitted.
5. H. Rabbel, M. Werner, J.-U. Sommer, Interactions of amphiphilic triblock copolymers with lipid membranes, Mode of interaction and effect on permeability examined by generic Monte-Carlo simulations, manuscript in preparation.
6. A. Czogalla, E. P. Petrov, D. J. Kauert, V. Uzunova, Y. Zhang, R. Seidel and P. Schwille, Switchable domain partitioning and diffusion of DNA origami rods on membranes, *Faraday Discussion*, 2013, 161, 31.
7. A. Iltzsche, C. Kizil, A. K. Thomas, Y. Zhang, M. Brand, Efficient cargo delivery to parenchymal cells of the brain using a short cell-penetrating peptide, submitted.
8. S. M. Balko, F. Heinemann, J. Friedrichs, A. K. Thomas, Y. Zhang, P. Schwille, C. Werner, Topography of ultra-thin biohybrid hydrogel films effects lipid diffusion and contact angles of DOPC giant vesicles, to be submitted.
9. M. Thompson, M. Tsurkan, K. Chwalek, M. Bornhauser, M. Schlierf, C. Werner, Y. Zhang, Self-assembling hydrogels crosslinked solely by receptor-ligand interactions: tunability, rationalization of physical properties and 3D cell culture, submitted.
10. M. Thompson, R. Wieduwild, R. Reddavid, M. Tsurkan, H. Andrade, C. Werner, Y. Zhang, Kinetic-controlled hydrogel formation based on protein-ligand interaction, Patent application, Register number: 102014104566.1.
11. R. Wieduwild, S. Krishnan, K. Chwalek, A. Boden, C. Werner, Y. Zhang, Non-covalent matrix beads as microcarriers for cell culture, *Angew. Chem.*, under revision.
12. R. Wieduwild, M. Tsurkan, K. Chwalek, P. Murawala, M. Nowak, U. Freudenberg, C. Neinhuis, C. Werner, Y. Zhang, Minimal peptide motif for non-covalent peptide-heparin hydrogels, *J. Am. Chem. Soc.*, 2013, 135, 2919.

13. R. Wieduwild, Y. Zhang, C. Werner, M. Tsurkan, U. Freudenberg, Minimal peptide sequence motifs for the design of self-assembled oligosaccharide-polymer hydrogels, Patent application, PCT register number: PCT/DE2013/100327, pending patent number WO 2014/040591.
14. S. M. Balko, A. K. Thomas, Y. Zhang, C. Werner, Cell penetrating peptides induce adhesion changes in giant vesicles on ultra-thin biohybrid gel films, to be submitted.
15. R. Wieduwild, W. Lin, A. Boden, K. Kretschmer, Y. Zhang, A repertoire of peptide tags for controlled drug release from injectable non-covalent hydrogel, *Biomacromol.*, 2014, 15, 2058.
16. M. Tsurkan, R. Wetzal, H. Pérez-Hernández, K. Chwalek, A. Kozlova, U. Freudenberg, G. Kempermann, Y. Zhang, A. Lasagni, C. Werner, Photopatterning of multifunctional hydrogels to direct adult neural precursor cells, *Adv. Healthc. Mater.*, 2014, in press.
17. N. Sakai, S. Matile, Anion-mediated transfer of polyarginine across liquid and bilayer membranes, *J. Am. Chem. Soc.*, 2003, 125, 14348-14356.
18. N. Sakai, T. Takeuchi, S. Futaki, S. Matile, Direct observation of anion-mediated translocation of fluorescent oligoarginine carriers into and across bulk liquid and anionic bilayer membranes, *ChemBioChem.*, 2005, 6, 114.
19. N. Sakai, S. Futaki, S. Matile, Anion hopping of (and on) functional oligoarginines: from chloroform to cells, *Soft Matter*, 2006, 2, 636-641.
20. S. M. Balko, M. Werner, A. K. Thomas, Y. Zhang, J.-U. Sommer, C. Werner, Improving translocation of cell penetrating peptides by design: computer simulation and experiment, to be submitted.
21. M. Carido, Y. Zhu, K. Postel, B. Benkner, P. Cimalla, M. O. Karl, T. Kurth, F. Paquet-Durand, E. Koch, T. A. Munch, E. M. Tanaka, M. Ader, Characterization of a mouse model with complete RPE loss and its use for RPE cell transplantation, *Invest. Ophth. Vis. Sci.*, 2014, 55, 5431.
22. A. Meinhardt, E. Eberle, A. Tazaki, A. Ranga, M. Niesche, M. Wilsch-Bräuninger, A. Stec, G. Schackert, M. Lutolf, E. M. Tanaka, Three dimensional reconstitution of the patterned neural tube from embryonic stem cells, *Stem Cell Reports*, 2014, in press.
23. Y. Zhu, M. Carido, A. Meinhardt, T. Kurth, M. O. Karl, M. Ader, E. M. Tanaka, Three-dimensional neuroepithelial culture from human embryonic stem cells and its use for quantitative conversion to retinal pigment epithelium, *PLoS One*, 2013, 8, e54552.
24. Y. Zhu, E. M. Tanaka, Method for producing polarized retinal progenitor cells from pluripotent stem cells and their differentiation into retinal pigment epithelium cells, European patent application no. EP10161354.5.
25. Y. Zhu, E. M. Tanaka, Method for producing polarized retinal progenitor cells from pluripotent stem cells and their differentiation into retinal pigment epithelium cells, US patent application no. 13/096,598.